RSC Advances

ROYAL SOCIETY OF CHEMISTRY

www.rsc.org/advances

TiO_2 replica of ZnO nanosheets were synthesized, showing exceptional e-transport properties in dye solar cells.

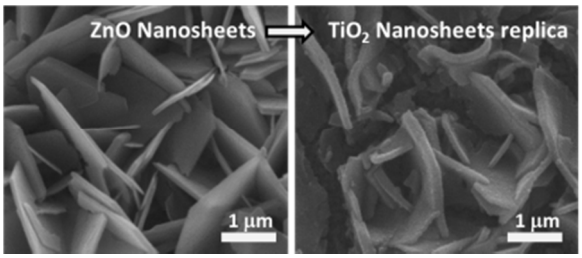

Cite this: DOI: 10.1039/c0xx00000x

www.rsc.org/xxxxxx

Paper

Nanosheet arrays of TiO_2 synthesized by one step conversion of ZnO nanosheets: Boosting of electron transport rate and application in dye solar cells

Sara Alimirsalari[a], Fariba Tajabadi[b*], S. Mohsen Salehkoutahi[a], Raheleh Ghahary[c] and Nima Taghavinia[d*]

Received (in XXX, XXX) XthXXXXXXXXX 20XX, Accepted Xth XXXXXXXXX 20XX
DOI: 10.1039/b000000x

A TiO_2 replica of ZnO nanosheet films is synthesized using a chemical replacement process. ZnO nanosheets are grown by electrodeposition on fluorine doped tin oxide (FTO) films, and a dissolution/deposition process is used to convert the ZnO template into a TiO_2 replica. Electron microscopy shows the final TiO_2 structure follows the morphology of the initial ZnO template. X-ray diffraction and energy dispersive spectroscopy verify the total transformation of ZnO to TiO_2. The as synthesized TiO_2 sheets are amorphous and after annealing turn to anatase phase. The film of TiO_2 nanosheets is used as the photoanode of a dye sensitized solar cell. Despite the low roughness factor of 100, a conversion efficiency of 3.3% with D35 as sensitizer is achieved. The nanosheets show remarkably faster electron transport and longer electron lifetime compared to the conventional TiO_2 nanoparticle electrodes.

Introduction

Titanium dioxide remains one of the most important semiconductor materials, with wide range of research activity around it. Different properties such as wide band gap, high chemical stability, environmentally friendly nature, and low cost, make TiO_2 applicable in photovoltaics, photocatalysis, and chemical sensors.[1-5]In most of these potential applications, the morphology of TiO_2 plays an important role in determining the performance of devices.

In case of sensitized solar cells, including dye- and quantum dot-sensitized solar cells, the structures of the TiO_2photoelectrodes greatly affect the cell performance. Various morphology parameters, including roughness factor, grain boundaries, crystallinity and light scattering influence the dye loading, electron transport time, electron lifetime and finally cell efficiency.[6-11]Mesoporous structures based on TiO_2 nanoparticles is the conventional structure for dye solar cells(DSC). In these structures the transport time is relatively large, limiting the device to work only with certain electrolyte compositions that provide longer electron lifetime. One and two dimensional structures are expected to provide faster electron transport by geometrically limited transport paths.[12, 13]In depleted heterojunction quantum dot solar cells, the surface area of the mesoporous TiO_2 is not important, while electron transport properties is critical. For these cells it has been demonstrated that one dimensional structures show better electron transport rate and higher efficiency compared to planar structures.[14]

The template-assisted method is a universal approach to design and prepare certain nanostructures that cannot be directly grown because of specific crystal habits. Different TiO_2 morphologies have been fabricated using templates, by growing TiO_2 and subsequent removing of the template.[15-17]Contrary to TiO_2, ZnO nanostructures with different morphologies can be easily obtained depending on the preparation method. ZnO structures can be a good template for preparation of one and two-dimentional TiO_2 nanostructures. Electrodeposition of ZnO in controlled conditions has been reported to yield one and two dimensional morphologies on fluorine doped tin oxide (FTO) surface.[18-24]The power conversion efficiencies obtained in ZnO-based DSCs are typically significantly lower compared to TiO_2-based devices. Therefore ZnO structures are preferred as templates that may yield TiO_2 with certain one or two dimensional structures. There are reports on using liquid phase deposition of $TiO_2$by TiF_4 on ZnO nanorodes, resulting in a composite of TiO_2-ZnO nanostructures.[14,25] In a recent work, TiO_2 is deposited on ZnO nanosheets and ZnO is removed in the next step, to create hollow structures of TiO_2.[26]

In this research, we present a one step method to fabricate films of TiO_2nanosheets from ZnO nanosheets deposited on FTO surface. A dissolution/deposition process has been employed to convert ZnO nanosheets into TiO_2 nanosheets. ZnO nanosheets were fabricated by electrochemical deposition method. The final product was used as the photoanode of DSC devices. These TiO_2 nanosheet electrodes exhibit significantly better electron transport properties.

Experimental Section

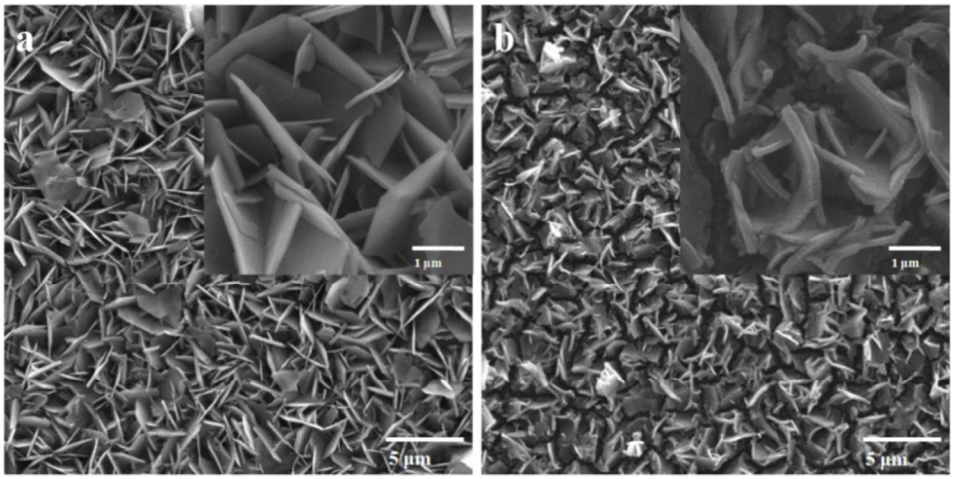

Fig.1 SEM images of initial ZnOnanosheets array of FTO substrate **(a)** and converted TiO_2nanosheets**(b)**

***Preparation of ZnO template*:**Films of ZnO nanosheets have been prepared by electrochemical deposition in a three-electrode glass cell immersed in a water bath held at 70°C. The working and counter electrodes were FTO/glass substrates (15Ω/cm^2, Dyesol), while an Ag/AgCl electrode was used as the reference electrode. An aqueous solution of 0.05M $Zn(NO_3)_2$•$6H_2O$ (Merck) mixed with 0.1M KCl (Merck) as the supporting electrolyte have been used for the electrodeposition. A potentio/galvanostat electrochemical workstation (PalmSense) was used to deposit the nanostructures by amperometery potentiostatic method at -1.1 V (relative to the Ag/AgCl electrode) and for different deposition times. After the deposition, the resulting films were thoroughly rinsed with deionised (DI) water. The prepared films were annealed at 350°C for 30 min.

***Synthesis of TiO_2nanosheets*:** The synthesized ZnO nanosheet films on FTO were immersed vertically in an aqueous solution consisting of 0.05M of $(NH_4)_2TiF_6$ (Aldrich) and 0.15M of H_3BO_3 at 28°C for 0-120 min, while the solution has been stirred slowly. The pH of the solution was set at 4.15. It has been explored that in this situation, $(NH_4)_2TiF_6$is hydrolyzed and then condensed as TiO_2 on the surface of individual ZnO nanosheets while ZnO is dissolved simultaneously in the acidic solution produced by $(NH_4)_2TiF_6$ hydrolysis. In other words, $Zn^{2+}$is exchanged with Ti^{4+} and $TiO_2$is deposited in place of ZnO. The TiO_2 films were rinsed with DI water, then immersed in ethanol and then pentane each for 5 min, and finally drying at room temperature. TiO_2films were crystallized in air at 500°C for 60 min.

Fabrication and Characterization of DSCs: Dyeing of the prepared films were performed in either a 0.4mMethanolic solutions containing cis-bis(isothiocyanato)bis(2,2′-bipyridyl-4,4′-dicarboxylato)-ruthenium(II)bis-tetrabutylammonium dye (N719, Solaronix) or DN-F04(E)-3-(5-(4-(Bis(20,40-dibutoxybiphenyl-4-yi) amino)thiophene-2-yl)-2- cyanoacrilyc acid (D35) at room temperature for different times. The sensitized films were rinsed with ethanol for removing the excess dye molecules remaining on the surface. Subsequently, the sensitized electrode was sandwiched together with a platinum-coated FTO as the counter electrode separated by about 30 μm Surlyn spacer. The internal space between two electrodes was filled with an electrolyte solution composed of 0.1M LiI, 0.1M I_2, 0.5M 4-tert-butylpyridine and 0.6M methylhexylimidazolium iodide in acetonitrile by capillary action. The active area of the resulting cell exposed in light was 0.25 cm^2. For comparison, conventional TiO_2 nanoparticle electrodes (20 nm, 12μm thick, Sharif Solar paste) were prepared in identical fabrication conditions. The DSC performance was evaluated in AM1.5 simulated light (Sharif Solar) using a potentiostat/galvanostat (IVIUM, Compact stat) workstation.

In order to estimate the internal surface area of the films, the number of dye molecules adsorbed on the film was measured by dye de-loading in an aqueous 0.1 M NaOH solution. The concentration of dye in the solution was determined by monitoring its absorption peak using UV-Vis spectrometry (Perkin Elmer Lambda-25). The size of a dye molecule has been assumed 1.5 nm^2.

The morphology and composition of the films were recorded using scanning electron microscopy (SEM Philips, XL30) equipped with EDS analyzer. The crystal structure of layers was analyzed by X-ray diffraction patterns (XRD, X'Pert Pro MPD, PAnalytical).IMPS and IMVS spectra were measured by Modulight (Ivium) coupled to Compactstat (Ivium). The white LED (425-660 nm) of Modulight at a constant luminous flux of 42.75 lm and amodulation amplitude of 10 % of the bias illumination was employed for both intensity-modulated photocurrent spectroscopy (IMPS) andintensity modulated photovoltage spectroscopy (IMVS) measurements.

Results and Discussions

Fig. 1a shows the top view of ZnO nanosheets grown on the substrate, which exhibit regular hexagonal-end plates with about 70 nm thickness. It can be observed that the surface of ZnO nanosheets is smooth, so the roughness factor is very low. Also it shows that the ZnO nanosheets grow vertically on the substrate. These ZnO nanosheets were used as templates and were subsequently converted to TiO_2 nanosheets(Fig. 1b) via a one step dissolution/deposition process. The following reactions are involved in this dissolution/deposition process:[24,27]

$$TiF_6^{2-} + 2H_2O \rightarrow TiO_2 + 6F^- + 4H^+$$

$$H_3BO_3 + 4HF \rightarrow HBF_4 + 3H_2O$$

$$ZnO + 2H^+ \rightarrow Zn^{2+} + H_2O$$

ZnO nanosheets dissolve into the solution by reacting with H_3O^+ which provides proper condition for the hydrolysis of $TiF_6^{2-}$and subsequent condensation as deposited TiO_2. As shown in Fig. 1b, TiO_2nanosheets nearly follow the original ZnO template structure, however with higher thickness (100-140nm). Also the surface of TiO_2 sheets is not as smooth as the original ZnO sheets, and the sheets are slightly bent. Bending could be attributed to stress build-up in the sheets in the process of chemical conversion and sintering. Similar effect has been observed for hollow porous TiO_2 nanosheets.[26]

The process of conversion of ZnO sheets to TiO_2 sheets involves a controlled balance between the dissolution of ZnO, and sol-gel deposition of TiO_2 in place of ZnO. This balance occurs at certain pH, Ti precursor concentration and bath temperature. There have been reports of similar processes involving fabrication of TiO_2nanorod or nanotube from ZnO nanorod template.[28-30]During this dissolution/ deposition process, the cation exchange reaction between Zn^{2+} and Ti^{4+} ions occurs, which could be qualitatively understood in terms of hard–soft acid–base theory.[31] Because Ti^{4+} is a harder acid compared to Zn^{2+}, Ti^{4+} could bind strongly with the O^{2-} anion to form TiO_2. The conversion of ZnO to $TiO_2$is strongly favoured due to a thermodynamic driving force of about -249kJmol^{-1}.

EDS data of Zn and Ti contents of the ZnO and TiO_2nanosheets were recorded at different times of the conversion process. The average contents of Zn and Ti as a function of time during the conversion process are shown in Table1. This indicates that the deposition of TiO_2 and removal of ZnO proceed simultaneously. It is noted that after 90 min all zinc content of initial ZnO layer has been removed, while about 90% of Zn is removed after about 10 min of reaction.

Fig. 2 shows the XRD patterns of the ZnO and TiO_2nanosheet films before and after annealing process. After annealing, ZnO film shows a hexagonal structure. The diffraction peaks at 31.77º, 34.45º and 36.28º are indexed as ZnO lattice planes (100), (002) and (101), respectively (JCPDS 01-079-0207). The XRD pattern of as prepared ZnO nanosheets is presented in Fig. 2b, which indicates diffraction peaks of ITO and hexagonal ZnO as well as some diffraction peaks which could not be indexed to any compound in the Powder Diffraction File (PDF).As it can be seen in the XRD spectra, TiO_2nanosheets are in the anatase phase and the diffraction peaks at 25.28º, 38.28º, 48.08º, 55.18º, and 62.78º were observed, which corresponded to the (101), (103), (200), (211), and (204) planes of TiO_2anatase phase, respectively (JCPDS 01-086-1157). No ZnO diffraction peaks were observed, suggesting that ZnO was completely converted to TiO_2 after the chemical transformation.

Nanosheetfilms of ZnO and TiO_2 were used as photoanodes for fabricating DSCs. Fig. 3 shows the current density versus voltage characteristics of the fabricated DSCs. The photovoltaic performance of the fabricated cells are listed in Table 2. TiO_2 nanosheets show clearly improved performance compared to the original ZnO nanosheet DSCs. For N719 dye, the conversion efficiency for ZnO nanosheet DSC is 0.46%, while for TiO_2 nanosheets, the efficiency is increased to 2.4%. For D35 dye, the TiO_2 cells exhibits slightly higher efficiency of 3.31%. These efficiencies are less than the efficiency of conventional nanoparticle TiO_2 DSCs. This is due to the considerably smaller roughness factor of the nanosheets.

V_{oc} of the ZnO device is considerably lower than TiO_2 devices, as clearly observed in Figure 3a. This is an indication that there is less accumulation of charge in ZnO compared to TiO_2. Figure 3b displays the data of charge extraction measurements for both ZnO and TiO_2 devices. The data represents also the charge density as the morphology of the films is almost the same. One observes that for the same V_{oc}, ZnO devices show higher extracted charge density. Alternatively, for identical extracted charge density, TiO_2 devices result in higher Voc. This indicates that at open circuit condition, a larger part of the charge is lost via recombination in case of ZnO, compared to TiO_2. The recombination problem in ZnO DSCs is a known effect, which is mainly attributed to dissolution of ZnO in dye solution and precipitation of Zn-dye complexes on the surface.[32,33]

The ZnO based solar cells show lower performance compared to TiO_2 cells. Different reasons can be mentioned for it including the dissolution of ZnO and the formation of dye−Zn^{2+} aggregates,[32,33] lower injection efficiency,[32,33]lower dye regeneration efficienc[33] and increased surface trap density after the dye adsorption.[34] Because of the dye−Zn^{2+} aggregates, a large amount of inactive dye molecules remains in the film after the dye loading process, hence it is not possible to estimate the internal surface area by

Table .1 Zn and Ti contents averaged along the depth versus ZnO-to-TiO_2 conversion time analysed by EDAX.

Deposition time (min)	*Zn(%)*	*Ti (%)*
0	100	0
7	12.5	87.5
15	4.2	95.8
30	2.8	97.2
60	2.7	97.3
90	0	100
120	0	100

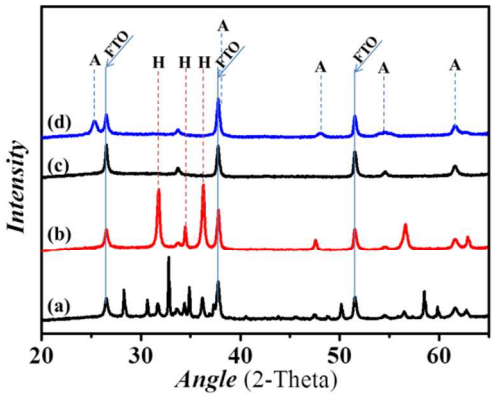

Fig. 2 XRD patterns of as prepared ZnO nanosheets (**a**), annealed ZnO nanosheets (**b**), as prepared TiO_2 nanosheets (**c**) and annealed TiO_2 nanosheets (**d**).

Table 2 Photovoltaic performance of the DSCs based on ZnO and TiO_2 nanosheet photoelectrodes.

Structure	*Sensitizer*	V_{oc} *(V)*	J_{sc} *(mA/cm²)*	*FF* %	η %
ZnO nanosheets	N719	0.62	1.56	48	0.46
TiO_2 nanosheets	N719	0.79	4.37	70	2.42
TiO_2 nanosheets	D35	0.78	7.33	58	3.31

dye loading and de-loading method. However, this method can be used for TiO_2 nanosheets, where a roughness factor of 100 is obtained for the TiO_2 nanosheet film. This roughness factor is very low in comparison with the roughness factor of conventional mesoporous photoanodes (about 1000). By using a dye with higher extinction coefficient (D35, extinction coefficient=30000) higher current density and better conversion efficiency can be obtained with these low surface area nanosheet electrodes.

IMVS and IMPS data were used for electron lifetime and electron transport time measurements. Fig. 4a shows the electron lifetime data versus the open circuit voltage. At a specific voltage, ZnO nanosheets exhibit the shortest lifetime, which may be explained by intensified recombination pathways in ZnO electrodes.[30]

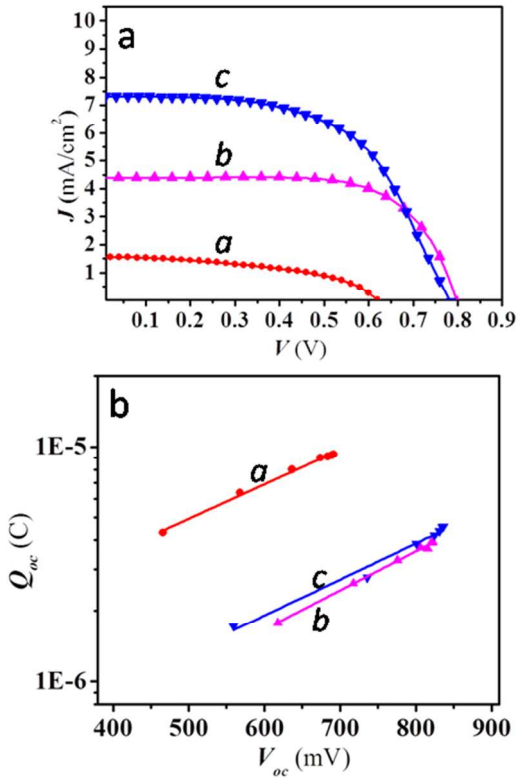

Fig. 3 (a) *J-V* characteristics of DSCs based on ZnO-nanosheets with N719 dye(a) TiO_2 - nanosheets with N719 dye (b) and TiO_2 nanosheets with D35 dye (c). **(b)** Extracted charge as a function of open- circuit voltage for the same solar cells.

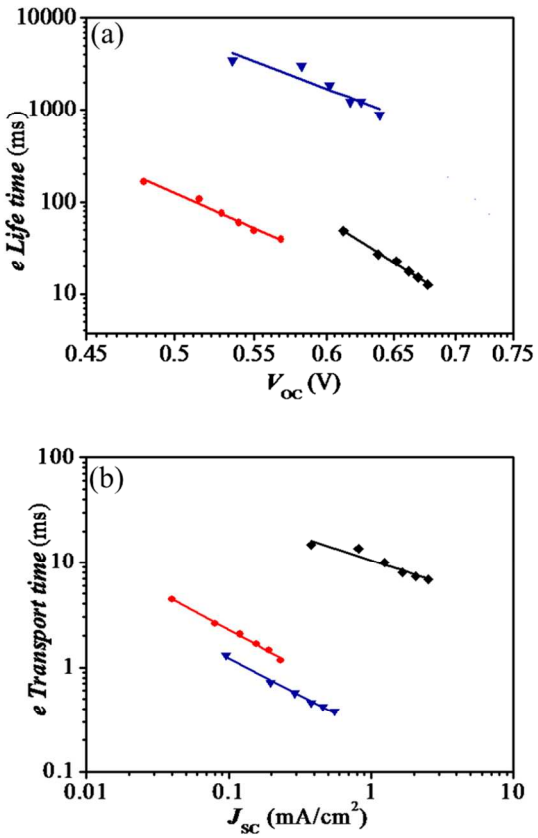

Fig. 4 Electron lifetime (a) and electron transport time (b) as determined by IMVS and IMPS measurements for DSCs fabricated from ZnO nanosheets (●) TiO_2 nanosheets (▼) and TiO_2 nanoparticles photoanode (♦).

TiO_2 nanoparticle electrodes show slightly better lifetime, while lifetime values for TiO_2nanosheet electrodes is significantly longer. This enhancement can be due to lower surface area (about 10 times smaller), lower trap density and also band bending in nanosheets due to relatively high sheet thickness.[31] Fig. 4b displays the electron transport time for the electrodes. ZnO and TiO_2 nanosheets show considerably better transport time compared to the conventional nanoparticle electrode.TiO_2 nanosheets exhibit even slightly better performance compared to ZnO nano sheets. As pointed out in the literature, ZnO is superior to TiO_2 as regards to bulk conductivity, where the conductivity is not much affected by traps, defects, and grain boundaries. In contrast, the electron diffusion coefficients measured for nanostructured ZnO devices are similar or inferior to those encountered for nanostructured TiO_2.[36] Since electrodeposited ZnO structures are polycrystalline after annealing a better electron transport is not expected. This is an evidence for better transport properties of lower dimensional structures, which can confine the electrons to more directional random walk pathways, compared to the three dimensional random walk transport in the conventional electrodes.

Conclusions

A simple one-step method for the synthesis TiO_2 nanosheet films is introduced. The process involves electrochemically grown ZnO nanosheets as the initial template, and a dissolution/deposition process to replace ZnO with TiO_2. This creates a TiO_2 replica of the ZnO nanosheets. The formed TiO_2nanosheets are Zn-free, and amorphous. They can be crystallized by heat treatment to be used as DSC electrodes. Despite the low roughness factor of 100, a conversion efficiency of 3.31% with D35 as sensitizer is achieved. The nanosheets show considerably better electron transport properties compared to the conventional nanoparticle electrodes. This opens opportunities for use of nanosheets in solar cell devices which do not require large surface area, such as colloidal quantum dot and perovskite solar cells.

Acknowledgements

We gratefully acknowledge the financial support of this work by Iranian Nanotechnology Initiative.

Notes and references

[a] *Physics Department, KhajeNasir University of Technology, P.O. Box 15418-49611, Tehran, Iran*
[b] *Nanotechnology and Advanced Materials Department, Materials and Energy Research Center, Karaj 31787-316, Iran, Email: tajabadi@ncl.sharif.edu,*
[c] *Sharif Solar Group, Sharif University of Technology, Tehran 14588, Iran,*
[d] *Physics Department and Institute for Nanoscience and Nanotechnology, Sharif University of Technology, Tehran 14588, Iran, Fax: + 98-21-6616 4119; Tel: +98-21-6616 4570, Email; taghavinia@sharif.edu*

† Electronic Supplementary Information (ESI) available: [Photovoltaic performance of the DSCs based on ZnO and TiO_2 nanosheet photoelectrodes with different films thickness and different dyes and electrolytes]. See DOI: 10.1039/b000000x/

‡ Footnotes should appear here. These might include comments relevant to but not central to the matter under discussion, limited experimental and spectral data, and crystallographic data.

1- X. Chen and S. S. Mao, *Chem. Rev.,* 2007, **107**, 2891-2959.
2- G. K. Mor, O. K. Varghese, M. Paulose, K. Shankar and C. A. Grimes, *Sol. Energy Mater. Sol. Cells*, 2006, **90**, 2011-2075.
3- P. V. Kamat, *J. Phys. Chem. C*, 2012, **116**, 11849-11851.
4- D. Chen and R. A. Caruso, *Adv. Funct. Mater*., 2012, **22**, 1966-1971.
5- R. Daghrir, P. Drogui and D. Robert, *Ind. Eng. Chem. Res*., 2013, **52**, 3581-3599.
6- N. Tetreault and M. Gratzel, *Energy Environ. Sci.*,2012,**5**,8506-8516.
7- Q. Zhang and G. Cao, *J. Mater. Chem*.,2011,**21**, 6769.
8- I. Mora-Ser,S. Gimnez, F. Fabregat-Santiago, R. Gmez, Q. Shen, T. Toyoda and J. Bisquert,*Acc. Chem. Res*., 2009, **42**, 1848-1857.
9- M. Gratzel, *Acc. Chem. Res*., 2009, **42**, 1788-1798.
10- G. Boschloo, A. Hagfeldt, L. Sun, L. Kloo and H. Pettersson, *Chem. Rev*., 2010, **110**, 6595 –6663.
11- S. Rhle, M. Shalom, A. Zaban, *ChemPhysChem*, 2010, **11**, 2290-2304.
12- P. Docampo, S. Guldin, T. Leijtens, N. K. Noel, U. Steiner, H. J. Snaith, Adv. Mater., 2014, DOI: 10.1002/adma.201400486.
13- Q. Zhang, G, Cao, *Nano Today*, 2011, **6**, 91- 109.
14- X. Lan , J. Bai , S. Masala , S. M. Thon , Y. Ren , I. J. Kramer , S. Hoogland , A. Simchi , G. I. Koleilat , D. Paz-Soldan , Z. Ning , A. J. Labelle , J. Young Kim , G. Jabbour and E. H. Sargent, *Adv. Mater*. 2013, **25**, 1769-1773.
15- E. Ghadiri, N. Taghavinia, S. M. Zakeeruddin, M. Gratzel, J. E. Moser, *Nano Lett*., 2010, **10** , 1632–1638.
16-S. Dadgostar, F. Tajabadi, N. Taghavinia, *ACS Appl. Mater. Interfaces,* 2012, **4**, 2964 – 2968
17- W. Kim, S. Y. Choi, Y. M. Jeon, S-k. Lee, S. H. Kim, *ACS Appl. Mater. Interfaces*, 2014, DOI: 10.1021/am502137d
18- F. Xu, Y. Lu, Y. Xie, Y. Liu, *Mater Design*, 2006, **30** 1704–1711
19- F. Xu, M. Dai,Y. Lu, L. Sun, *J. Phys. Chem. C,* 2010, **114**, 2776–2782
20- O. Lupan, V.M. Guérin, I.M. Tiginyanu, V.V. Ursaki, L. Chow, H. Heinrich, T. Pauporté, *J. Photochem. Photobiol. A: Chem*., 2010, **211** 65–73
21- H. Chen, L. Zhu, M.Wang, H. Liu, W. Li, *Nanotechnology,* 2011, **22** 475402
22- H. Chen, W. Li, H. Liu, L. Zhu, *Electrochem. Commun.*, 2011, **13**331–334
23- H. Chen, L. Zhu, H. Liu, W. Li, *Thin Solid Films*, 2013, **534**, 205–213
24- H. Chen, L. Zhu, H. Liu, W. Li, *Electrochim. Acta*.,2013, **105**, 289–298
25- J. Tian, Q. Zhang, E. Uchaker, Z. Liang, R. Gao, X. Qu, S. Zhangand G. Cao, *J.Matter. Chem. A*, 2013,**1**, 6770-6775.
26- H. Chen, L. Zhu, Q. Hou, H. Liu and W. Li, *ChemSUSChem*, 2013, **6**, 983-988.
27- S. Yodyingyong, X. Y. Zhou, Q. F. Zhang, D. Triampo, J. T. Xi, K. Park, B. Limketkai and G. Z. Cao, *J. Phys. Chem. C*, 2010, **114**, 21851-21855.
28- S-I. Na, S-S. Kim, W-K. Hong, J-W. Park, J. Jo,Y-C. Nah, T. Lee, D-Y. Kim, *Electrochim. Acta,* 2008,**53**, 2560–2566
29- X. Lan, J. Bai, S. Masala, S. M. Thon,Y. Ren, I. J. Kramer, S. Hoogland, A. Simchi, G. I. Koleila, D. Paz-Soldan, Z. Ning, A. J. Labelle, J. Y. Kim, G. Jabbour, E. H. Sargent, *Adv. Mater.,* 2013, **25**, 1769–1773
30- J-H. Lee, I-C. Leu, M-C. Hsu, Y-W. Chung, M-H. Hon,*J. Phys. Chem. B,*2005, **109**, 13056-13059
31- S. Muduli, O. Game, V. Dhas, A. Yengantiwar, S. B. Ogale, *Energy Environ. Sci.,* 2011, **4**, 2835-2839.
32- H. Horiuchi, R. Katoh, K. Hara, M. Yanagida, S. Murata, H. Arakawa and M. Tachiya,*J. Phys. Chem. B,* 2003, **107**, 2570−2574.
33- M. Quintana, T. Edvinsson, A. Hagfeldt, G. Boschloo,*J. Phys. Chem. C*, 2007, **111**, 1035−1041.
34- J. J. Wu, G. R. Chen, H. H. Yang, C. H. Ku and J. Y. Lai,*Appl.Phys. Lett.,* 2007, **90**, 213109.
35- H. Ogawa, M. Nishikawa, A. Abe, *J. Appl. Phys*., 1982, **53**, 4448–55
36- J. Phys. Chem. C 2012, 116, 11413−11425